Activation of CO_2 on copper surfaces : the synergy between electric field, surface morphology, and excess electrons

Activation of CO_2 on Copper Surfaces: The Synergy between Electric Field, Surface Morphology and Excess Electrons

Amin Jafarzadeh, Kristof M. Bal, Annemie Bogaerts and Erik C. Neyts*

Research group PLASMANT, Department of Chemistry, University of Antwerp,

Universiteitsplein 1, 2610 Wilrijk-Antwerp, Belgium

ABSTRACT

In this work we use DFT calculations to study the combined effect of external electric fields, surface morphology and surface charge on CO_2 activation over Cu (111), Cu (211), Cu (110) and Cu (001) surfaces. We observe that the binding energy of the CO_2 molecule on Cu surfaces rises significantly upon increasing the applied electric field strength. In addition, rougher surfaces respond more effectively to the presence of the external electric field towards facilitating the formation of a carbonate-like CO_2 structure and the transformation of the most stable adsorption mode from physisorption to chemisorption. The presence of surface charges further strengthens the electric field effect and consequently gives rise to an improved bending of the CO_2 molecule and C-O bond length elongation. On the other hand, a net charge in the absence of externally applied electric field shows only a marginal effect on CO_2 binding. The chemisorbed CO_2 is more stable and further activated when the effects of an external electric field, rough surface and surface

charge are combined. These results can help to elucidate the underlying factors that control CO_2 activation in heterogeneous and plasma catalysis, as well as in electrochemical processes.

1. Introduction

Due to the alarming amount of greenhouse gas emissions in recent years and their widely believed impact on the climate, the need for finding more efficient and novel ways to mitigate these effects is felt more than ever. Efficient conversion of CO_2 as the major produced greenhouse gas to value-added chemicals, such as hydrocarbons and alcohols, and thus reducing the anthropogenic carbon emission, would not only facilitate a sustainable way to tackle environmental issues caused by global industrialization, but also will help to revamp renewable energy resources.[1–3]

Cu surfaces have been widely used for the purpose of CO_2 reduction. However, it is known that activation and further reduction of CO_2 over Cu surfaces is not straightforward without the help of electro-catalytic conditions, e.g., an applied external potential and corresponding occurrence of electric fields and charges in the electrochemical double layer. For instance, Chernyshova et al[4] showed that a clean Cu (111) surface in the presence of an aqueous electrolyte is not able to activate CO_2 without the presence of a relaxed Na^+ cation hydrated by eight water molecules on top of the linear CO_2 molecule. Also, Garza et al[5] concluded that the formation of a negative carbonate-like structure of CO_2 on Cu (111) in an electrolyte medium is not favorable until the effect of the applied electrochemical potential is considered. Indeed, applied potentials can lead to significant changes in the thermodynamics of catalytic reactions: It has been reported that electric fields stronger than $0.1\ V/\text{Å}$ can alter the energies of molecular orbitals of adsorbates,[6,7] which in turn leads to changing chemisorption patterns, as well as different activation energies of reactions over metal surfaces.

Although electrochemical systems have shown successful performance towards CO_2 reduction over metal catalysts, accurate simulation of the interface between the electrodes and an electrolyte is highly challenging mostly because of the existence of complex electrolyte environment and limitations for applying the electrochemical potential [8]. It is known that explicit approaches used for elucidation of the electrolyte are computationally demanding[9]. On the other hand, it is difficult to assess the accuracy of the description for the solid-liquid interface using implicit methods that treat the electrolyte medium using continuum models[9].

Moreover, in an electrochemical double layer as found in the electrochemical activation of CO_2, many phenomena potentially contributing to the reaction are taking place at the same time (e.g. electric fields, excess electrons, solvent molecules, solvated ions, changes in surface morphology, etc). As a result, it is very difficult to pinpoint the precise effect of each individual phenomenon or understand if and how any synergies between them can arise. For this reason, it would be useful to alternatively study a pure gas-facing system to focus on the respective roles of the field and excess electrons, and not take any electrolyte into account. Not only does such a set-up dramatically simplify the surface physicochemistry—and thus allow for a more focused exploration of the role of excess electrons and electric fields—but it is also a physically sensible model of certain phenomena arising at a plasma–catalyst interface.

Indeed, a plasma provides a non-equilibrium and reactive environment for chemical reactions, thanks to the ions, electrons, radicals and (vibrationally and electronically) excited species present [10]. The plasma can also affect a catalyst, for example by generating strong electric fields near the surface, or by depositing excess electrons. In contrast to electrochemical systems, where electric field and charge distributions are intertwined phenomena that directly depend on the applied potential and nature of the electrolyte solution, these effects can vary significantly in plasma setups, which means that a potentially much more diverse chemistry can be accessed[20]. In addition, the Debye length in common plasmas is typically in the order of μm or larger (as opposed to nm

in electrochemical systems). Therefore, the electronic effect of the double layer can easily be incorporated in microscopic models in the form of a net charged slab and external electric field without the need to take into account solvent molecules or specific microscopic countercharge distributions. Thus, a simple model of a gas-facing catalyst also represents a true physical aspect of a plasma-catalytic setup, besides being of purely theoretical interest.

Using density functional theory (DFT) calculations, we have already shown that the presence of excess electrons improves the activation of CO_2 on supported transition metal clusters [21,22]. In these works, however, we did not attempt to disentangle the role of electric field and surface charge. In the present study, we therefore systematically assess the respective contributions of electric fields and excess charges on well-defined catalytic copper surfaces. Moreover, by considering different surface facets we can also reveal how the morphology of the catalyst controls the response of the surface chemistry to any of these electronic effects.

In this study, we developed methodologies to efficiently study the effect of external electric fields and excess electrons on molecular adsorption. First, we will consider the effect of the two different electronic effects in isolation and evaluate the role of the surface structure. Subsequently, we will simultaneously consider the electric field and excess electrons and we will explain how their combined effect can improve the activation of CO_2 over Cu surfaces with different morphologies. Besides its direct relevance to the understanding of surface chemistry in plasma catalysis, our results also provide fundamental insights into charge-based phenomena as found in electrochemical systems.

2. Computational Details

All calculations are performed on four different Cu surfaces ((111), (211), (110) and (001)) by means of density functional theory (DFT) calculations. A lattice constant of 3.615 Å[24] is used for making the slabs. The (111), (110) and (211) surfaces consist of four atomic layers, while we chose

five layers for the more compact structure of (001). Further details, including dimensions of the supercell used for each slab, are provided in the supporting information (SI).

The Quickstep[25] module of the CP2K[26] package is used for all calculations, employing molecularly optimized (MOLOPT)[27] double–ζ valence plus polarization (DZVP) basis sets, together with an auxiliary plane wave basis set with $800\ Ry$ cutoff for the expansion of Kohn-Sham orbitals. Electron exchange and correlation effects are dealt with using the general gradient approximation (GGA) Perdew-Burke-Ernzerhof (PBE)[28] functional, while applying Grimme's D3 approximation together with Becke-Johnson damping for dispersion corrections[29,30]. Inner shell electrons are taken into account by using Goedecker-Teter-Hutter (GTH) pseudopotentials,[31,32] while for the upper shell electrons of Cu, C and O we consider 11, 4 and 6 valence electrons, respectively. Geometry optimizations are performed using the Broyden-Fletcher-Goldfarb-Shanno (BFGS) scheme with a maximum relaxation force tolerance of $0.02\ eV/\text{Å}$ between atoms. Partial charges on atoms are achieved using the Hirshfeld-I scheme[33] as implemented in CP2K. We performed test calculations both with k-point sampling of the Brillouin zone by using $4 \times 4 \times 1$ Monkhorst-Pack mesh[34] and k-point sampling which was limited to the Γ–point only. We found that sampling with the Γ–point only is significantly faster compared to k-point sampling with $4 \times 4 \times 1$ Monkhorst-Pack mesh, while there are only minor differences in adsorption energies and all the trends stayed the same. We therefore carried out the calculations considering sampling of the Brillouin zone restricted to the Γ–point only. Full periodic calculations are performed along the surface (only x and y directions) in order to avoid unrealistic interactions with replicated pictures along the z direction[35].

For modeling the electric field effect, we use two different methods: a constant potential method for the field-only effects and the charged plates (or dipole sheet) method for considering the combined effects of electric field and excess electrons. As we will show in the following paragraphs, both methods are capable of yielding equivalent energetics for the field-only

calculations, but only the latter can be used in systems carrying a net charge. In this study, the direction of the electric field in all calculations is chosen to be normal to the surface of the metal slab and in $-\vec{Z}$ direction. So, all the positive numbers reported here for the electric field represent its absolute value or strength.

The constant potential method is based on using an implicit (generalized) Poisson solver[23] by employing Dirichlet boundary conditions to simulate the applied voltage on the system without using dipole sheets. The main advantage of using Dirichlet boundary conditions is that this method makes it possible to directly apply a specified potential, together with the elimination of the need for considering large supercells. Also, it maintains the neutrality of the supercell during the calculations. In the charged plates approach, we use a dipole sheet with some modifications to include the combined effect of the electric field and the excess electrons. This method requires localized (atom-centered) basis sets and is thus not applicable in packages using plane-waves only. In this approach, we use two charged plates as electrodes and we employ the Martyna-Tuckerman (MT) Poisson solver[36]. Charged plates consist of atomic cores with modified charges in a way that both plates are charged with opposite signs, making a dipole sheet in the middle of the simulation box. Using this novel technique has made it possible to fine-tune the amount of charge on the plates and the corresponding electric field strength between dipole sheets. In case of considering the combined effect of an electric field and one excess electron, we can add one unit of implicit extra charge to the system together with the charged plates. A schematic picture of the both abovementioned methods is provided in Figure 1.

Using the constant potential approach, the electric field strength on a conductor surface depends on the distance between the electrodes and correspondingly on the thickness of the metal slab $\left(E = \frac{\Delta \mathrm{V}}{D-d}\right)$; in which, E is the field strength, $\Delta \mathrm{V}$ is the potential difference, D is the distance between the electrodes and d is the slab thickness. This makes it feasible to consider a change in

electric field strength due to the morphology and the thickness of the surface. In other words, depending on the thickness and roughness of the used slab, the strength of the electric field arising from a specific potential would be different.

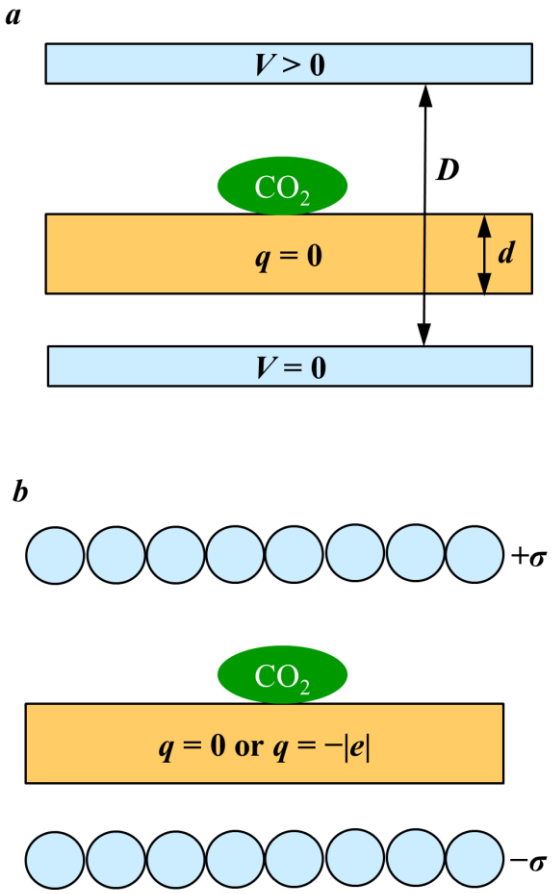

Figure 1- a) Constant potential method used for "field only" effect and b) Dipole sheet method used for combined effect of charge and external field on CO_2 activation over Cu surfaces

Using the dipole sheets approach, the strength of the electric field between the charged plates is given by ($E = \frac{\sigma}{\varepsilon_0}$) in which σ is the surface charge density of the dipole sheet and ε_0 is the vacuum permittivity. Thus, the distance between the charged plates and thickness of the slab does not affect the strength of the electric field achieved. However, the charged plates cannot be placed too close to the slab, to avoid explicit interactions with the dummy ions in the plates.

In order to compare Cu (111) (with thickness of 6.26 Å) to Cu (110) (with thickness of 8.77 Å) surfaces, we used Dirichlet boundaries to apply a $15\,V$ potential difference on the electrodes, resulting in different electric field strengths for each slab ($1.08\,V/\text{Å}$ for Cu (111) and $1.31\,V/\,\text{Å}$ for Cu (110)). Making the same comparison using charged plates with applying the charge density of 0.089 $\frac{C}{m^2}$ on dipole sheets, we get the same electric field strength for both surfaces ($1.00\,V/\text{Å}$ for Cu (111) and $1.01\,V/\text{Å}$ for Cu (110)). In other words, using a fixed setup in the case of the Dirichlet boundaries results in different external field strength when applied to different slabs, which must be accounted for when comparing different surface morphologies. For methodological consistency, we have opted to use the same electrode settings for all considered surface slabs in all further calculations using Dirichlet boundaries. The main disadvantage of the method is that it is not possible to combine the electric field effect with the effect of excess electrons since the method assumes charge neutrality.

Despite these differences between both approaches, we can obtain equivalent results using both methods, provided that we correct for the different slab size dependencies of both methods; details of this cross-checking are provided in the SI. Adsorption energies are achieved as the subtraction of gas-phase CO_2 and bare slab total energies from the complex (surface + adsorbed molecule) total energy. In order to be consistent with the experiments, we have considered CO_2 in gas-phase without the presence of an electric field, while taking into account the energies of the bare slab and complex in the presence of an electric field. In this case, the CO_2 molecule is initially outside of the area influenced by the field and once it arrives, it starts to get affected by the applied electric field while approaching the surface. Deshlahra et al. have used the same approach for the study of CO chemisorption on Pt (111) in the presence of a uniform electric field[37].

3. Results and discussion

We first report on the calculations done using constant potential electrodes, which are meant to investigate the effect of an external electric field on bare Cu surfaces and their ability to adsorb CO_2. Next, we will shortly report on the effect of net charges without the presence of an external electric field. Finally, by using the modified dipole sheet method we will discuss the combined effect of electric field and excess electrons on the redistribution of surface charges on pristine Cu surfaces and on CO_2 chemisorption patterns.

3.1 Electric field effect using constant potential electrodes

CO_2 adsorption on all Cu surfaces is studied first without an applied potential and then compared with the results achieved in the presence of a negative electric field. The applied voltage range is between 0 and $25\,V$. Note that extreme potentials over $25\,V$ lead to very strong electric fields, such that CO_2 gets dissociated and attached to the upper electrode, which results in unphysical energies. Also in most cases above $25\,V$, Cu atom detachment from the surface is seen as a result of 'field-evaporation'. This effect has already been reported as the detachment of single atoms and even clusters from metal surfaces in response to applying very strong electric fields to the system[38,39].

3.1.1 Electric field effect on bare surfaces

We started with applying a potential on the upper electrode while keeping the lower electrode at zero potential, to see how this changes the electrostatic potential inside the simulation box for bare Cu surfaces. As expected without the applied electric field, the potential rapidly falls to zero after a short distance from both sides of the surfaces. In this case, negative partial surface charges of the top and bottom layers are present, showing a slight charge accumulation over the surfaces of the metal slab. After applying an electric field to the bare surface, the charge distribution inside the surface changes in a way that leads to a migration of negative charge from the bottom to the above

layers of the slabs (opposite to the electric field direction). The linear relationship between the electric field strength and the charge separation over the top and bottom layers of the surface is shown in Figure S2. The slope of the potential in both upper and lower sides of the metal surface resulted in the same electric field strength, considering the zero-field inside the conductor slab (Figure S3). This is in excellent agreement with the potential distribution reported by Deshlahra et al[37].

3.1.2 Electric field effect on CO_2 adsorption

Without the presence of an applied electric field, CO_2 does not chemisorb on Cu surfaces, no matter how rough the surface is. In all cases without applied electric field, physisorbed CO_2 is the most stable structure on the Cu surfaces, which is consistent with literature[40–42]. Corresponding adsorption energies and bond lengths and angles for CO_2 adsorption on Cu surfaces upon changing the applied potential are shown in the SI (Tables S3 – S6).

On Cu (111), physisorption stays as the most stable mode until the applied electric field reaches a value of around $1\ V/\text{Å}$, when chemisorption becomes the favored mode. Figure 2 shows the most stable adsorption mode of CO_2 over the Cu surfaces as a function of the applied potential to the upper electrode. For the $\Delta V = 15\ V$ case, the slight increase in adsorption energy is due to improved Coulomb interaction between the carbon atom of the slightly bent molecule and the negative surface charge. Bending of the molecule is a natural result of the force applied to the positive carbon atom towards the electric field, while pushing negatively charged oxygen atoms in the opposite direction. Once the adsorption mode changes from physisorption to chemisorption, there is a dramatic change in the adsorption energy and C-O bond elongation, together with a decrease in O-C-O angle, which all point to the CO_2 activation. We have also studied the change in accumulated charge of the molecule as a result of increasing the applied potential. Figure 3

shows a linear relationship between the strength of the applied electric field and the increase in the accumulated charge on the adsorbed CO_2 over all Cu surfaces.

Note that considering the different thickness of the slabs, the applied voltages will lead to slightly different external electric fields at the slab surface. This is shown in Figures 4 and 5. Even though the applied potential is the same, the strength of the electric field is different for each slab configuration.

On Cu (211), as one of the rough surfaces that we have considered, CO_2 gets weakly chemisorbed with an adsorption energy of $-0.33\ eV$ when applying a potential of $5\ V$ (equivalent to $0.41\ V/\text{Å}$ electric field strength) (see Figures 4 and 5). By increasing the applied potential, the adsorption energy increases together with the improved C-O bond elongation and accumulated charge in comparison to the Cu (111) surface. As shown in Figure 5, at the voltage of $25\ V$, corresponding to an electric field of $1.94\ V/\text{Å}$, we have a strong adsorption energy of $-1.96\ eV$ together with the longest C-O bond length and smallest O-C-O angle.

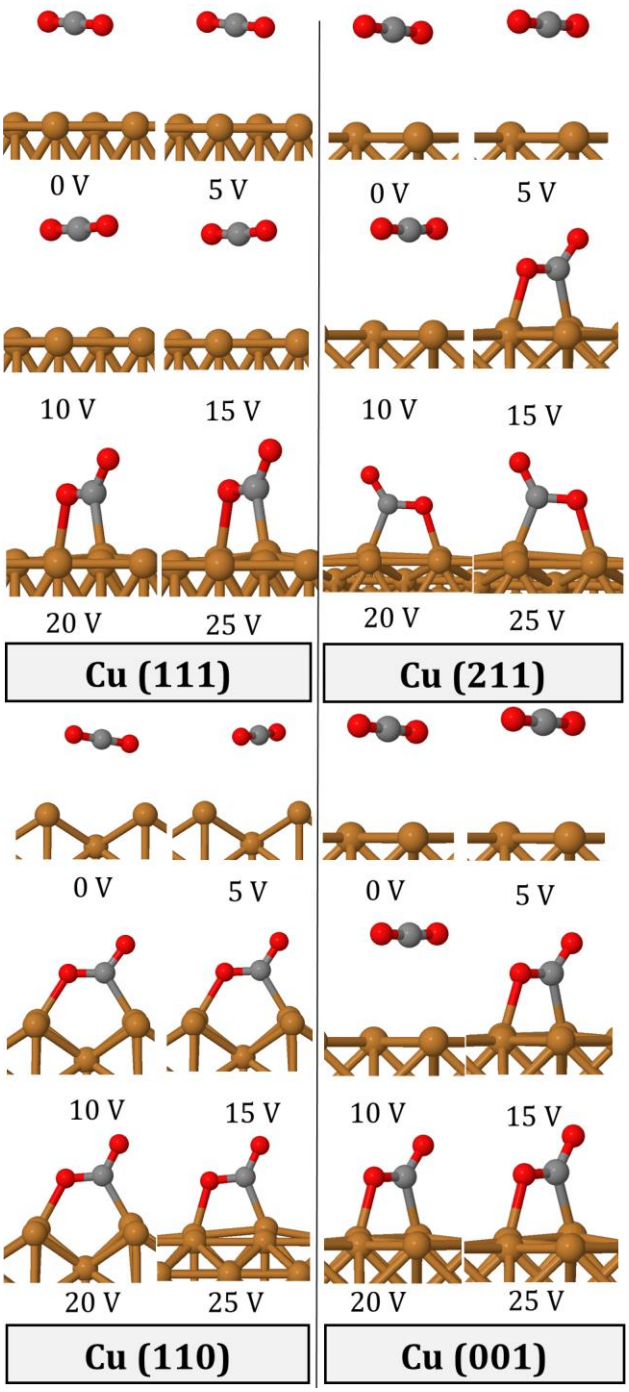

Figure 2-The most stable CO_2 adsorption mode on Cu surfaces for different applied potentials.

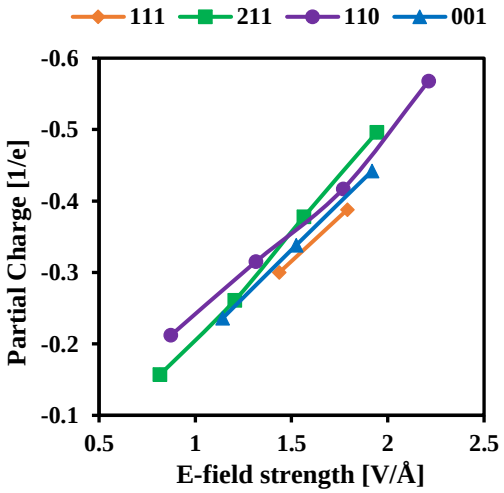

Figure 3- Partial charges of the adsorbed CO_2 Vs E-field strength.

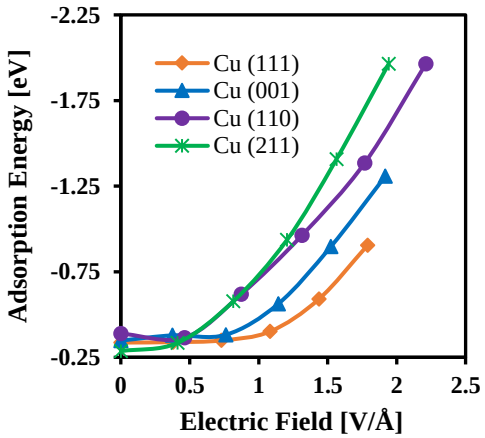

Figure 4- Adsorption energy of CO_2 over Cu surfaces as a function of the electric field strength between both electrodes.

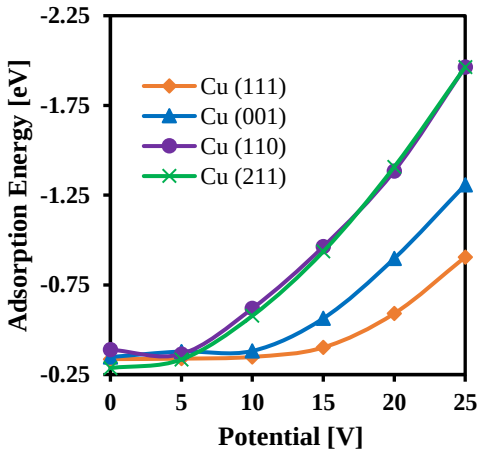

Figure 5- Adsorption energy of CO_2 over Cu surfaces as a function of the applied potential between both electrodes

CO_2 adsorption patterns over Cu (110) are more or less similar to the (211) case with this difference that the physisorption to chemisorption transformation occurs after applying a somewhat larger potential to the system. As shown in Figure 2, CO_2 prefers a long-bridge site for chemisorption for the applied voltage range of 5 to 20 V. However, for the $\Delta V = 25\ V$ case we found the most stable chemisorbed CO_2 on a short-bridge site. From Figure 5 it can be seen that at 25 V applied potential, the adsorption energy is the same as on the Cu (211) surface, together with the consistent results with bond elongation and increase in negative partial charge of the molecule.

The Cu (001) slab shows a stronger response to the electric field towards CO_2 chemisorption in comparison to the other flat surface (Cu (111)). In the presence of an applied electric field, chemisorbed CO_2 is more stable on (001) surfaces than on (111). This higher sensitivity is seen also in the larger partial charge accumulation on the CO_2 molecule as a result of the presence of the electric field (Figure 3). A detailed look into the projected density of states (PDOS) of both slabs reveals the underlying reason for the difference in performance. Only strong electric fields lead to a very small shift in the surface *d* states towards the valence band. However, this shift is more pronounced in the molecule's *s* or *p* states. Figures 6 and 7 show the PDOS of both surfaces

upon changing the applied potential. As indicated by the blue arrows, shifting of the C and O states for the CO_2 adsorbed on (001) surface is more noticeable in comparison to the (111) slab. This improved shifting leads to enhanced hybridization between the molecule and the metal surface states. This can also apply to the observed change in performance of Cu (211) and Cu (110) surfaces. More details on the bonding properties between CO_2 and Cu atoms are provided in the SI.

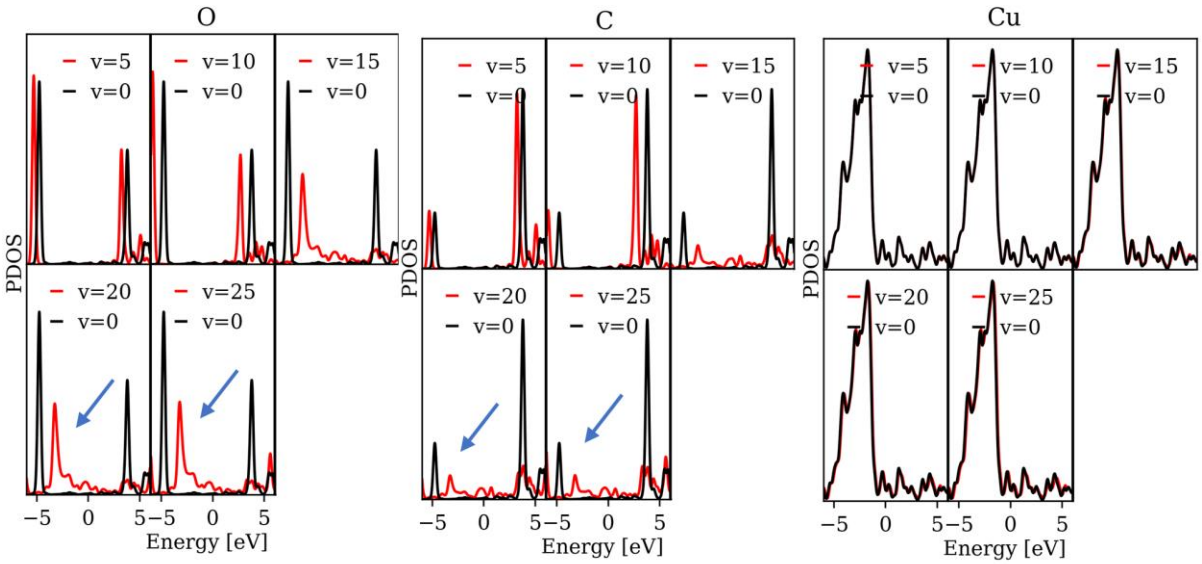

Figure 6- Projected density of states for CO_2 adsorption on Cu (001)

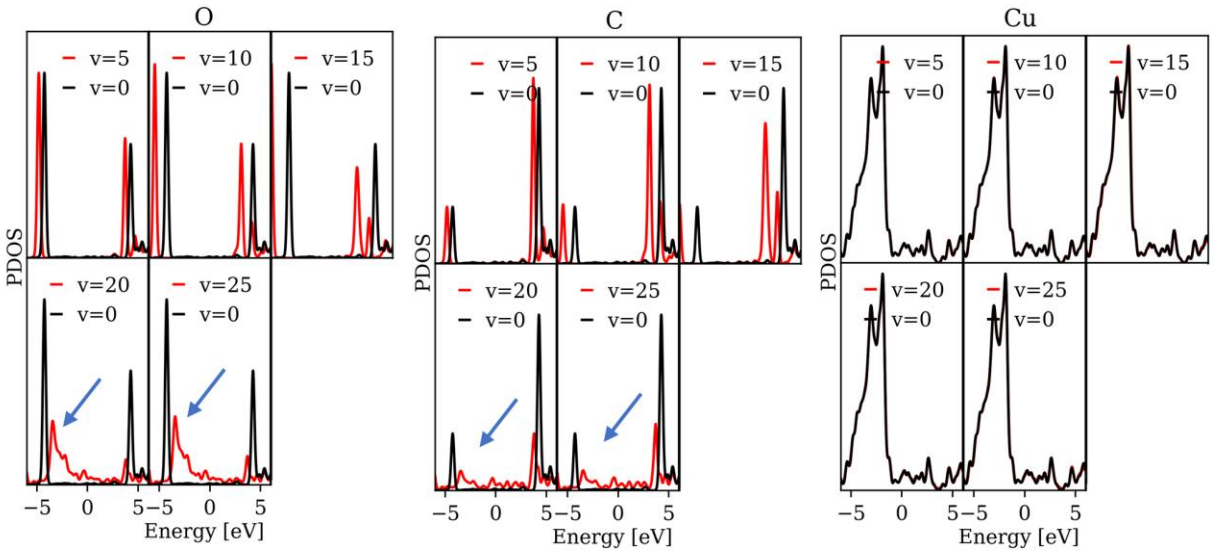

Figure 7- Projected density of states for CO_2 adsorption on Cu (111)

In summary, the results indicate that a negative electric field has a strong impact on the adsorption of CO_2 and more specifically on its chemisorption as the first step towards activation. The rougher surfaces respond more strongly to the electric field. This is partially because of the local electric field enhancements as a result of morphological differences. Also, less coordinated atoms in rougher surfaces, like (211) and (110), are more prone to make a stable bond with CO_2 than the highly coordinated Cu atoms in flatter surfaces.

3.2 Excess electron effect on CO_2 adsorption patterns

In order to make a consistent comparison between the individual effect of each parameter and the combined effects, we also need to consider the presence of excess electrons only, without any external electric field applied to the system. In this case, we first optimized the CO_2 adsorption (using both initially physisorbed and chemisorbed configurations) on all surfaces without any charge or electric field applied. Then we re-optimized the most stable structure by adding one electron to the system. We found that the lone added charge gets evenly distributed on both sides of the slab, as expected from electrostatic theory, and does not lead to any noticeable change in the adsorption energy of the molecule. In all cases the re-optimized structure with the excess electron has almost the same stability as the neutral structure (with differences in adsorption energies less than $0.02\ eV$, as shown in Figure 8.

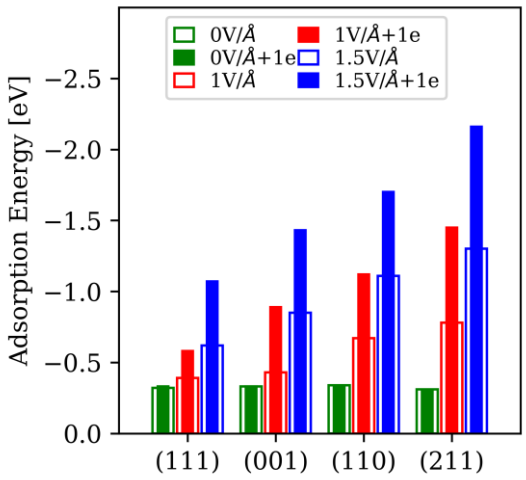

Figure 8- Adsorption energy of CO_2 on Cu surfaces as a function of both electric field and excess electrons

For the Cu (110) surface without excess electron, same as the other surfaces, the most stable structure is the linear physisorbed CO_2. Once the excess electron is added, chemisorption becomes the most stable adsorption mode, although the adsorption energy increases as $0.01\ eV$. In other words, on the negatively charged surface of Cu (110), the physisorption mode is less stable than the chemisorption mode, in contrary to the neutral case. For all the other surfaces, the most stable neutral and re-optimized charged structures are linear physisorbed CO_2. These results show that without the presence of an external electric field the presence of excess electrons has a negligible effect on the adsorption properties of CO_2 on the Cu surfaces studied here. This is in line with our recent findings for CO_2 chemisorption on charged semiconductors; there, the adsorption enhancement due to the presence of excess electrons is linearly correlated with the work of charging or, more generally, the band gap[43]. As a result, the chemistry on metallic surfaces can also be expected to be mostly unaffected by negative charging.

3.3 Combined electric field and excess electrons using the modified dipole sheet approach

We have devised a modified version of the dipole sheet approach to be able to explain the combined effects occurring in plasma catalysis as a result of an electric field and plasma-induced excess electrons. As in the previous section, we first study the combined effects on bare surfaces and then extend it to the adsorption of CO_2 over Cu surfaces.

3.3.1 Combined effect on bare surfaces

Using a dipole sheet induces a uniform electric field between the plates independent of the thickness of the employed metal surface. This is different from the case of the constant potential electrodes approach in which the electric field strength varies with the size of the vacuum area between electrodes (which changes when metal surfaces with different thicknesses and morphologies are placed between the electrodes). In order to apply the intended electric field between the dipole sheets, the electric charge on the plates should be adjusted. Tables S1 and S2 in the SI show values for charge and surface charge density for the corresponding strengths of the external electric field.

Once we add an excess electron to the system together with applying the electric field, the distribution of the electrons on both upper and lower surfaces of the slab will be changed. This will lead to altered electric fields in the regions on the top and bottom of the metal slab, as it is seen from the results that the slope of the potential in cases with the combined effect of electric field and excess electron is different in the upper and lower regions of the slab (Figure S9). Also, it is seen that the presence of an excess electron increases the accumulated partial negative charges on both sides of the slab (Figure S8). This makes the upper layer more negative and the bottom layer less positive, which in turn increases/decreases the electric field strength in the upper/lower vacuum regions of the metal slab. This effect is more pronounced by using a stronger electric field, which increasingly leads to charge separation on both sides of the slab.

3.3.2 Combined effect on CO_2 adsorption

In order to study the combined effect of electric field and plasma-induced excess electron on CO_2 adsorption over Cu surfaces, we employ two electric field strengths ($1V/\text{Å}$ and $1.5V/\text{Å}$), both with and without adding excess electrons, and we compare the results. In the presence of the electric field only, the results are entirely in agreement with the results achieved by the constant potential electrode approach. The most stable configurations for CO_2 adsorption over Cu surfaces in presence of combined electric field and excess electrons are provided in the SI (Figures S4 – S7). For the case of Cu (111), without adding an excess electron, $1V/\text{Å}$ electric field is not sufficient to induce chemisorption (Figure S4), while as shown in Figures S5 – S7, the chemisorbed phase of CO_2 is the most stable adsorption mode under the examined circumstances for all the other surfaces.

Adding one excess electron to the system together with applying the electric field gives rise to CO_2 creating a stable chemisorbed phase on Cu (111) and more stabilization of previously formed chemisorbed structure on the three other surfaces. By carefully analyzing the partial charges on the atoms involved in bonding (provided in the SI- Tables S11-S14) we realize that once the chemisorption occurs, the Cu atom coordinating with the C atom of the molecule attains a noticeable partial charge, while there is only marginal change in the partial charge of the other neighboring Cu atoms. This leads to the formation of a polar covalent bond, considering the positive partial charge of the C atom. This is the opposite for the Cu atom, which makes a bond with the O atom of the molecule. In this case, the previously negatively charged Cu atom loses all its charge to the bonded oxygen atom and remains slightly positive. The other oxygen atom of the molecule gets a pronounced partial negative charge, which indicates the further activation of the molecule.

In all cases, adding an excess electron leads to an improvement of the electric field effect, correspondingly giving rise to an increase in adsorption energy and C-O bond stretching and decrease in O-C-O bond angle. The trends in adsorption energy are shown in Figure 8. The combined effect of an electric field and excess electrons on the partial charges of the CO_2 molecule are displayed in Figure 9. We can achieve more or less the same results for the $\frac{1V}{\text{Å}} + 1e$ and $\frac{1.5V}{\text{Å}}$ cases, which implies that by combining the excess electrons with the electric field we can get the same results towards the CO_2 activation as a 50% stronger field.

As already seen in the previous section, Cu (211) shows the strongest binding ability amongst the four different slabs studied here. The same reasoning for the improved CO_2 activation can be used here, which stresses the important role of the surface morphology in response to the charge and electric field effect. By analyzing the PDOS (provided in the SI; Figures S10 – S13), the same shifting in s and p states of the CO_2 as a result of applying an electric field and excess electrons is also seen. By slightly shifting the metal's d states around the Fermi level, the increased accumulated negative charge on the upper layer of the slab also helps to further mixing between the surface and the molecule's states. The more negatively charged the surface, the stronger the bond it makes with the positive carbon atom of the molecule. In this situation, the repulsion between the negatively charged surface and the reduced oxygen atoms leads to further bending of the molecule. As shown in Figure 9, improved bent structures are accompanied by an increased accumulated partial charge on the CO_2 molecule.

Improved CO_2 activation due to the increased electric field (achieved by the combination of electric field and plasma-induced excess electrons) suggests that the electric field enhancement could be the key factor leading to the higher CO_2 conversion rates in plasma catalysis. In other words, fine-tuning the surface morphology of the catalyst together with the presence of excess

electrons could be employed to adjust the required electric field strength aiming for higher conversion rates.

These results also help to explain the role of excess electrons in electrochemical CO_2 reduction. Our initial results for the isolated effect of electric fields or excess electrons seem to suggest that the primary contributor to CO_2 chemisorption is the electric field, so that the only role of the excess electrons is that of a charge carrier needed to obtain the applied potential drop. However, whenever an electric field is present, the electrons in the surface will also play a chemical role, meaning that both have a direct effect on the chemistry. Due to the nature of electrochemical systems, with the applied potential drop within an electrolyte intertwining the two phenomena, such synergistic behavior is always present; it is only through the simplified systematic approach in our study that this precise entanglement can be characterized.

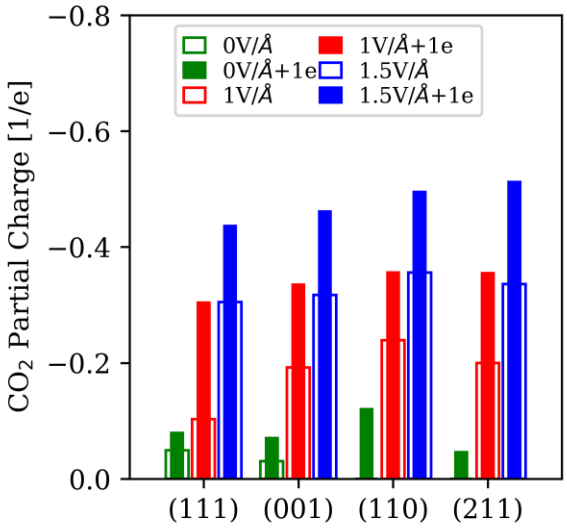

Figure 9- Partial charge of adsorbed CO_2 over different Cu surfaces

Conclusion

In this study, we have investigated the effect of an electric field, excess electrons, as well as the combination thereof, on CO_2 adsorption over Cu surfaces. We used a new technique based on

charged parallel plates, which enabled us to analyze for the first time the combined effect of electric field and excess electrons in a plasma-catalytic system. The results of this study reveal that an external negative electric field induces a switch from physisorption to chemisorption of the CO_2 molecule on Cu surfaces. This effect is even stronger when an excess electron is present in the system. In contrast, excess electrons without the presence of an external electric field have no appreciable effect on CO_2 binding. Overall, an increase in adsorption energies, partial charges and C-O bond elongations in CO_2 are seen due to applying the electric field with or without the presence of excess electrons.

We notice that the rougher surfaces respond more effectively to the presence of the electric field and excess electrons, which we attribute to the locally stronger fields and also less coordinated surface atoms in comparison to the highly coordinated atoms in flat surfaces.

Considering the various synergies that arise through the combined effects, controlling the surface roughness, charge deposition and electric field strength could be effective parameters to tune and optimize the CO_2 activation process over Cu surfaces.

Associated Content

The supporting information is available free of charge.

It contains information on: Information on the supercells used for the calculations, Details for making the dipole sheets, Cross-checking details, Potential and surface partial charge curves using constant potential and dipole sheet methods, Tables mentioning bond length, angles and adsorption energies for the most stable CO_2 adsorption mode as a function of various applied field/charge conditions, PDOS for combined electric field and excess electron effect, Hirshfeld charges of the surface atoms and adsorbed molecule using dipole sheet method.

Author information

Corresponding author

Email: amin.jafarzadeh@uantwerpen.be

Tell: +32-32652360

Fax: +32-32652343

Acknowledgment

The financial support from the TOP research project of the Research Fund of the University of Antwerp (grant ID: 32249) is highly acknowledged by the authors. The computational resources used in this study were provided by the VSC (Flemish Supercomputer Center), funded by the FWO and the Flemish Government – department EWI.

References:

(1) Song, J. T.; Song, H.; Kim, B.; Oh, J. Towards Higher Rate Electrochemical CO 2 Conversion: From Liquid-Phase to Gas-Phase Systems. *Catalysts*. MDPI AG March 1, 2019. https://doi.org/10.3390/catal9030224.

(2) Gao, D.; Zegkinoglou, I.; Divins, N. J.; Scholten, F.; Sinev, I.; Grosse, P.; Roldan Cuenya, B. Plasma-Activated Copper Nanocube Catalysts for Efficient Carbon Dioxide Electroreduction to Hydrocarbons and Alcohols. *ACS Nano* **2017**, *11* (5), 4825–4831. https://doi.org/10.1021/acsnano.7b01257.

(3) Reske, R.; Mistry, H.; Behafarid, F.; Roldan Cuenya, B.; Strasser, P. Particle Size Effects in the Catalytic Electroreduction of CO 2 on Cu Nanoparticles. *J. Am. Chem. Soc.* **2014**, *136* (19), 6978–6986. https://doi.org/10.1021/ja500328k.

(4) Chernyshova, I. V; Somasundaran, P.; Ponnurangam, S. On the Origin of the Elusive First Intermediate of CO2 Electroreduction. *Proc. Natl. Acad. Sci. U. S. A.* **2018**, *115* (40), E9261–E9270. https://doi.org/10.1073/pnas.1802256115.

(5) Garza, A. J.; Bell, A. T.; Head-Gordon, M. Is Subsurface Oxygen Necessary for the Electrochemical Reduction of CO2 on Copper? *J. Phys. Chem. Lett.* **2018**, *9* (3), 601–606. https://doi.org/10.1021/acs.jpclett.7b03180.

(6) Che, F.; Gray, J. T.; Ha, S.; Kruse, N.; Scott, S. L.; McEwen, J.-S. Elucidating the Roles of Electric Fields in Catalysis: A Perspective. *ACS Catal.* **2018**, *8* (6), 5153–5174. https://doi.org/10.1021/acscatal.7b02899.

(7) Kreuzer, H. J. Physics and Chemistry in High Electric Fields. *Surf. Interface Anal.* **2004**, *36* (56), 372–379. https://doi.org/10.1002/sia.1895.

(8) Steinmann, S. N.; Sautet, P. Assessing a First-Principles Model of an Electrochemical Interface by Comparison with Experiment. *J. Phys. Chem. C* **2016**, *120* (10), 5619–5623. https://doi.org/10.1021/acs.jpcc.6b01938.

(9) Gauthier, J. A.; Ringe, S.; Dickens, C. F.; Garza, A. J.; Bell, A. T.; Head-Gordon, M.; Nørskov, J. K.; Chan, K. Challenges in Modeling Electrochemical Reaction Energetics with Polarizable Continuum Models. *ACS Catal.* **2019**, *9* (2), 920–931. https://doi.org/10.1021/acscatal.8b02793.

(10) C. Neyts, E.; (Ken) Ostrikov, K.; K. Sunkara, M.; Bogaerts, A. Plasma Catalysis: Synergistic Effects at the Nanoscale. *Chem. Rev.* **2015**, *115* (24), 13408–13446. https://doi.org/10.1021/acs.chemrev.5b00362.

(11) Wang, Q.; Yan, B.-H.; Jin, Y.; Cheng, Y. Dry Reforming of Methane in a Dielectric Barrier

Discharge Reactor with Ni/Al2O3 Catalyst: Interaction of Catalyst and Plasma. *Energy & Fuels* **2009**, *23* (8), 4196–4201. https://doi.org/10.1021/ef900286j.

(12) Fridman, A. *Plasma Chemistry*; Cambridge University Press, 2008; Vol. 9780521847353. https://doi.org/10.1017/CBO9780511546075.

(13) Tu, X.; Whitehead, J. C. Plasma-Catalytic Dry Reforming of Methane in an Atmospheric Dielectric Barrier Discharge: Understanding the Synergistic Effect at Low Temperature. *Appl. Catal. B Environ.* **2012**, *125*, 439–448. https://doi.org/10.1016/j.apcatb.2012.06.006.

(14) Neyts, E. C. Plasma-Surface Interactions in Plasma Catalysis. *Plasma Chem. Plasma Process.* **2016**. https://doi.org/10.1007/s11090-015-9662-5.

(15) Mei, D.; Zhu, X.; Wu, C.; Ashford, B.; Williams, P. T.; Tu, X. Plasma-Photocatalytic Conversion of CO2 at Low Temperatures: Understanding the Synergistic Effect of Plasma-Catalysis. *Appl. Catal. B Environ.* **2016**, *182*, 525–532. https://doi.org/10.1016/j.apcatb.2015.09.052.

(16) Chen, G.; Godfroid, T.; Britun, N.; Georgieva, V.; Delplancke-Ogletree, M. P.; Snyders, R. Plasma-Catalytic Conversion of CO2 and CO2/H2O in a Surface-Wave Sustained Microwave Discharge. *Appl. Catal. B Environ.* **2017**, *214*, 114–125. https://doi.org/10.1016/j.apcatb.2017.05.032.

(17) Chen, G.; Georgieva, V.; Godfroid, T.; Snyders, R.; Delplancke-Ogletree, M. P. Plasma Assisted Catalytic Decomposition of CO2. *Appl. Catal. B Environ.* **2016**, *190*, 115–124. https://doi.org/10.1016/j.apcatb.2016.03.009.

(18) Paulussen, S.; Verheyde, B.; Tu, X.; De Bie, C.; Martens, T.; Petrovic, D.; Bogaerts, A.; Sels, B. Conversion of Carbon Dioxide to Value-Added Chemicals in Atmospheric Pressure

Dielectric Barrier Discharges. *Plasma Sources Sci. Technol.* **2010**, *19* (3). https://doi.org/10.1088/0963-0252/19/3/034015.

(19) Ma, X.; Li, S.; Ronda-Lloret, M.; Chaudhary, R.; Lin, L.; van Rooij, G.; Gallucci, F.; Rothenberg, G.; Raveendran Shiju, N.; Hessel, V. Plasma Assisted Catalytic Conversion of CO2 and H2O Over Ni/Al2O3 in a DBD Reactor. *Plasma Chem. Plasma Process.* **2019**, *39* (1), 109–124. https://doi.org/10.1007/s11090-018-9931-1.

(20) Bogaerts, A.; Zhang, Q. Z.; Zhang, Y. R.; Van Laer, K.; Wang, W. Burning Questions of Plasma Catalysis: Answers by Modeling. *Catal. Today* **2019**. https://doi.org/10.1016/j.cattod.2019.04.077.

(21) Jafarzadeh, A.; M. Bal, K.; Bogaerts, A.; C. Neyts, E. CO2 Activation on TiO2-Supported Cu5 and Ni5 Nanoclusters: Effect of Plasma-Induced Surface Charging. *J. Phys. Chem. C* **2019**, *123* (11), 6516–6525. https://doi.org/10.1021/acs.jpcc.8b11816.

(22) Bal, K. M.; Huygh, S.; Bogaerts, A.; Neyts, E. C. Effect of Plasma-Induced Surface Charging on Catalytic Processes: Application to CO2 Activation. *Plasma Sources Sci. Technol.* **2018**, *27* (2). https://doi.org/10.1088/1361-6595/aaa868.

(23) Bani-Hashemian, M. H.; Brück, S.; Luisier, M.; VandeVondele, J. A Generalized Poisson Solver for First-Principles Device Simulations. *J. Chem. Phys.* **2016**, *144* (4), 044113. https://doi.org/10.1063/1.4940796.

(24) Smura, C. F.; Parker, D. R.; Zbiri, M.; Johnson, M. R.; Gál, Z. A.; Clarke, S. J. High-Spin Cobalt(II) Ions in Square Planar Coordination: Structures and Magnetism of the Oxysulfides Sr2CoO2Cu2S 2 and Ba2CoO2Cu2S2 and Their Solid Solution. *J. Am. Chem. Soc.* **2011**, *133* (8), 2691–2705. https://doi.org/10.1021/ja109553u.

(25) Vandevondele, J.; Krack, M.; Mohamed, F.; Parrinello, M.; Chassaing, T.; Hutter, J. Quickstep: Fast and Accurate Density Functional Calculations Using a Mixed Gaussian and Plane Waves Approach. *Comput. Phys. Commun.* **2005**, *167* (2), 103–128. https://doi.org/10.1016/j.cpc.2004.12.014.

(26) Hutter, J.; Iannuzzi, M.; Schiffmann, F.; VandeVondele, J. Cp2k: Atomistic Simulations of Condensed Matter Systems. *Wiley Interdiscip. Rev. Comput. Mol. Sci.* **2014**, *4* (1), 15–25. https://doi.org/10.1002/wcms.1159.

(27) VandeVondele, J.; Hutter, J. Gaussian Basis Sets for Accurate Calculations on Molecular Systems in Gas and Condensed Phases. *J. Chem. Phys.* **2007**, *127* (11). https://doi.org/10.1063/1.2770708.

(28) Perdew, J. P.; Burke, K.; Ernzerhof, M. Generalized Gradient Approximation Made Simple. *Phys. Rev. Lett.* **1996**, *77* (18), 3865–3868. https://doi.org/10.1103/PhysRevLett.77.3865.

(29) Grimme, S.; Ehrlich, S.; Goerigk, L. Effect of the Damping Function in Dispersion Corrected Density Functional Theory. *J. Comput. Chem.* **2011**, *32* (7), 1456–1465. https://doi.org/10.1002/jcc.21759.

(30) Grimme, S.; Antony, J.; Ehrlich, S.; Krieg, H. A Consistent and Accurate Ab Initio Parametrization of Density Functional Dispersion Correction (DFT-D) for the 94 Elements H-Pu. *J. Chem. Phys.* **2010**, *132* (15). https://doi.org/10.1063/1.3382344.

(31) Krack, M. Pseudopotentials for H to Kr Optimized for Gradient-Corrected Exchange-Correlation Functionals. *Theor Chem Acc* **2005**, *114*, 145–152. https://doi.org/10.1007/s00214-005-0655-y.

(32) Goedecker, S.; Teter, M.; Hutter, J. Separable Dual-Space Gaussian Pseudopotentials. *Phys.*

Rev. B **1996**, *54* (3), 1703–1710. https://doi.org/10.1103/PhysRevB.54.1703.

(33) Bultinck, P.; Van Alsenoy, C.; Ayers, P. W.; Carbó-Dorca, R. Critical Analysis and Extension of the Hirshfeld Atoms in Molecules. *J. Chem. Phys.* **2007**, *126* (14), 144111. https://doi.org/10.1063/1.2715563.

(34) Monkhorst, H. J.; Pack, J. D. Special Points for Brillouin-Zone Integrations. *Phys. Rev. B* **1976**, *13* (12), 5188–5192. https://doi.org/10.1103/PhysRevB.13.5188.

(35) Bal, K. M.; Neyts, E. C. Modelling Molecular Adsorption on Charged or Polarized Surfaces: A Critical Flaw in Common Approaches. *Phys. Chem. Chem. Phys.* **2018**, *20* (13), 8456–8459. https://doi.org/10.1039/c7cp08209f.

(36) Martyna, G. J.; Tuckerman, M. E. A Reciprocal Space Based Method for Treating Long Range Interactions in Ab Initio and Force-Field-Based Calculations in Clusters. *J. Chem. Phys.* **1999**, *110* (6), 2810–2821. https://doi.org/10.1063/1.477923.

(37) Deshlahra, P.; Wolf, E. E.; Schneider, W. F. A Periodic Density Functional Theory Analysis of CO Chemisorption on Pt(111) in the Presence of Uniform Electric Fields. *J. Phys. Chem. A* **2009**, *113* (16), 4125–4133. https://doi.org/10.1021/jp810518x.

(38) Forbes, R. G. Field Evaporation Theory: A Review of Basic Ideas. *Appl. Surf. Sci.* **1995**, *87–88* (C), 1–11. https://doi.org/10.1016/0169-4332(94)00526-5.

(39) Sánchez, C. G.; Lozovoi, A. Y.; Alavi, A. Field-Evaporation from First-Principles. *Mol. Phys.* **2004**, *102* (9–10), 1045–1055. https://doi.org/10.1080/00268970410001727673.

(40) Muttaqien, F.; Hamamoto, Y.; Inagaki, K.; Morikawa, Y. Dissociative Adsorption of CO2 on Flat, Stepped, and Kinked Cu Surfaces. *J. Chem. Phys.* **2014**, *141* (3). https://doi.org/10.1063/1.4887362.

(41) Nakamura, J.; Rodriguez, J. A.; Campbell, C. T. Does CO2 Dissociatively Adsorb on Cu Surfaces? *J. Phys. Condens. Matter* **1989**, *1*. https://doi.org/10.1088/0953-8984/1/SB/026.

(42) Ou, L. Chemical and Electrochemical Hydrogenation of CO<inf>2</Inf> to Hydrocarbons on Cu Single Crystal Surfaces: Insights into the Mechanism and Selectivity from DFT Calculations. *RSC Adv.* **2015**, *5* (71), 57361–57371. https://doi.org/10.1039/c5ra09294a.

(43) Bal, K. M.; Neyts, E. C. Overcoming Old Scaling Relations and Establishing New Correlations in Catalytic Surface Chemistry: Combined Effect of Charging and Doping. *J. Phys. Chem. C* **2019**, *123* (10), 6141–6147. https://doi.org/10.1021/acs.jpcc.9b01216.

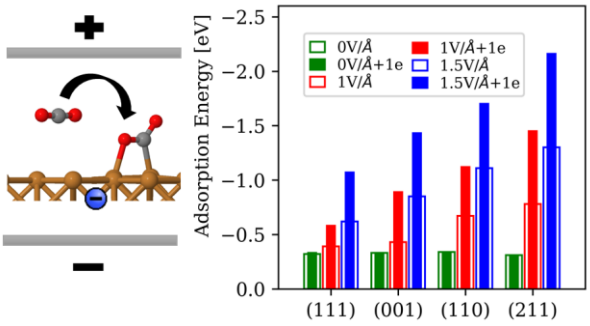

TOC Graphic